

Quantum fluctuation-driven first-order phase transitions in optical lattices

Boyang Liu¹ and Jiangping Hu^{1,2}

¹Beijing National Laboratory for Condensed Matter Physics, Institute of Physics, Chinese Academy of Sciences, Beijing 100190, China

²Department of Physics, Purdue University, West Lafayette, Indiana 47907, USA

(Received 13 June 2013; published 6 July 2015)

We study quantum fluctuation-driven first-order phase transitions of a two-species bosonic system in a three-dimensional optical lattice. Using effective potential method we find that the superfluid-Mott insulator phase transition of one type of bosons can be changed from second order to first order by the quantum fluctuations of the other type of bosons. The study of the scaling behaviors near the quantum critical point shows that the first-order phase transition has a different universality from the second-order one. We also discuss the observation of this phenomenon in the realistic cold-atom experiments based on the *in situ* density measurements.

DOI: [10.1103/PhysRevA.92.013606](https://doi.org/10.1103/PhysRevA.92.013606)

PACS number(s): 67.85.-d, 03.75.Mn, 05.30.Rt, 05.70.Jk

I. INTRODUCTION

Recently, the research of quantum criticality in cold-atom systems has attracted a great deal of interest. Several schemes have been proposed to determine the critical properties by extracting the universal scaling functions from the atomic density profiles [1–3]. The experimental observations of quantum critical behaviors of ultracold atoms have also been reported [4,5]. As a clean and highly controllable system, cold atoms can be a good playground to study various quantum critical behaviors.

An intriguing phenomenon near the quantum critical points (QCPs) is the effect of quantum fluctuation driven first-order phase transitions. The QCPs may become unstable in the appearance of competing orders. The nature of the phase transition can be changed from second to first order by the quantum fluctuations. This phenomenon was first discussed by Coleman and Weinberg [6]. They investigated a theory of a massless charged meson coupled to the electrodynamic field using effective potential method. Starting from a model without symmetry breaking at tree level they found that the one-loop effective potential indicated a new energy minimum appearing away from the origin. Independently, Halperin, Lubensky, and Ma [7] discovered the same phenomenon in the Ginzburg-Landau theory of superconductor to normal-metal transition and showed that the fluctuations of the electromagnetic field induce a first-order transition. Quantum fluctuation driven first-order phase transitions were also discussed in systems with multiple coupling constants [8,9]. Recently, there have appeared more examples of the nature of the quantum phase transition is predicted to become discontinuous as the QCP is approached [10–17].

In this paper we investigate the quantum fluctuation-driven first-order phase transitions of a two-species boson system in a three-dimensional optical lattice. This phenomenon has not been sufficiently explored in condensed-matter physics. With the recent progress in the research of the quantum critical behaviors in cold atom physics we are able to observe this phenomenon in a realistic experiment. Multicomponent bosonic systems have been studied both experimentally [18–21] and theoretically [22–29]. Compared with the paradigmatic superfluid to Mott insulator transition of a single-component Bose gas in an optical lattice [30–34], multicomponent bosonic systems have much richer phase diagrams. In our work

we implement Coleman and Weinberg's effective potential method [6] to calculate the quantum corrections to the classical action up to one-loop level. We find that the superfluid-Mott insulator phase transition of one type of bosons can be driven from second order to first order by the quantum fluctuations of the other type. We study the scaling behaviors near the first-order phase transition and give a feasible proposal to observe this phenomenon in cold-atom experiments.

II. TWO-SPECIES BOSE-HUBBARD MODEL

To describe Bose-Bose mixtures loaded into optical lattices, we consider the following two-species Bose-Hubbard Hamiltonian:

$$H = - \sum_{\alpha, \langle ij \rangle} t_{\alpha} (\hat{b}_{\alpha i}^{\dagger} \hat{b}_{\alpha j} + \hat{b}_{\alpha j}^{\dagger} \hat{b}_{\alpha i}) - \sum_{\alpha, i} \mu_{\alpha} \hat{n}_{\alpha i} + \sum_{\alpha, i} \frac{U_{\alpha}}{2} \hat{n}_{\alpha i} (\hat{n}_{\alpha i} - 1) + U_{AB} \sum_{i=1}^N \hat{n}_{1i} \hat{n}_{2i}. \quad (1)$$

Here $\hat{b}_{\alpha i}^{\dagger}$ creates a boson of sort $\alpha = A, B$ at site i . The first term in the Hamiltonian represents the hopping of bosons of types A and B between the nearest-neighbor pairs of sites $\langle ij \rangle$ with hopping amplitudes t_A and t_B . $\hat{n}_{\alpha i} \equiv \hat{b}_{\alpha i}^{\dagger} \hat{b}_{\alpha i}$ is the number operator of the α type boson at the site i . We have two chemical potentials μ_A and μ_B to fix the total number of type A and B bosons. U_{α} and U_{AB} denote the intra- and interspecies on-site interaction strengths.

The mean-field analysis shows that the system has three different phases [24]: (I) both species A and B stay in the superfluid phases, (II) one species is in the superfluid phase and the other one is in the Mott insulator phase, and (III) both species are in the Mott insulator phases. Two examples of the phase diagrams are shown in Fig. 1. To study the quantum fluctuation effects in the vicinity of QCPs we may take the limit of vanishing lattice constant and finally write down a continuum quantum field theory to describe the phase transitions. This can be done by following a standard procedure [35]: (I) writing the partition function in the coherent state path-integral representation, (II) decoupling the hopping terms by introducing two auxiliary fields φ_1 and φ_2 through the Hubbard-Stratanovich transformation, and (III) integrating out the fields b_{Ai}^{\dagger} , b_{Ai} , b_{Bi}^{\dagger} , and b_{Bi} . Then the action can be

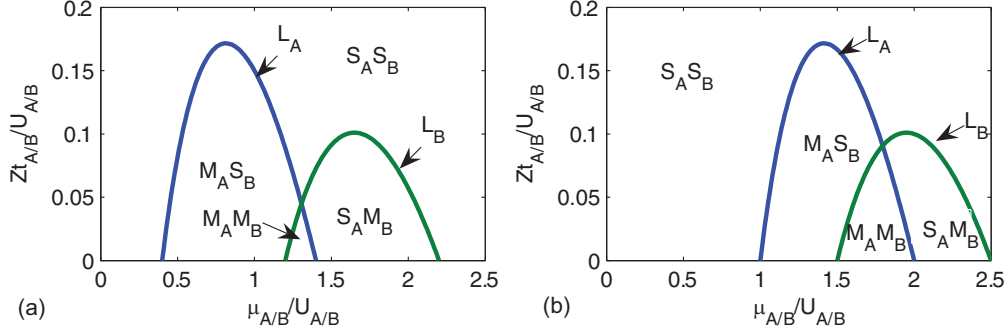


FIG. 1. (Color online) Phase diagrams of the two-species Bose-Hubbard model. The axes are either Zt_A vs μ_A or Zt_B vs μ_B , all in units of U_A or U_B , where Z is the number of the nearest neighbors around each lattice point. Curves L_A and L_B denote the superfluid-Mott insulator phase boundaries for species A and B . Depending on different parameters, L_A and L_B may divide the diagram into two, three, or four regions, two examples are presented here: (a) $n_1^0 = 1$, $n_2^0 = 2$, and $U_{AB}/U_A = U_{AB}/U_B = 0.5$; (b) $n_1^0 = 1$, $n_2^0 = 2$, and $U_{AB}/U_A = U_{AB}/U_B = 0.2$. Labels “ $S_A S_B$,” “ $M_A M_B$,” “ $S_A M_B$,” and “ $M_A S_B$ ” denote for superfluid phase for both species A and B , Mott insulator phase for both species A and B , superfluid phase for species A Mott insulator phase for species B , and superfluid phase for species B Mott insulator phase for species A .

written as

$$S = \int d\tau d^d x \left\{ u_1 \varphi_1^* \partial_\tau \varphi_1 + v_1 |\partial_\tau \varphi_1|^2 + w_1 |\nabla \varphi_1|^2 + u_2 \varphi_2^* \partial_\tau \varphi_2 + v_2 |\partial_\tau \varphi_2|^2 + w_2 |\nabla \varphi_2|^2 + r_1 |\varphi_1|^2 + r_2 |\varphi_2|^2 + \frac{g_1}{2} |\varphi_1|^4 + \frac{g_2}{2} |\varphi_2|^4 + g_3 |\varphi_1|^2 |\varphi_2|^2 \right\}. \quad (2)$$

The average of the two Hubbard-Stratanovich fields φ_1 and φ_2 are proportional to $\langle b_A(x, \tau) \rangle$ and $\langle b_B(x, \tau) \rangle$. Hence they can be taken as the superfluid order parameters. All the coefficients in Eq. (2) can be expressed in terms of the hopping amplitudes t_α , the chemical potentials μ_α , and the on-site interaction strengths U_α and U_{AB} ,

$$r_1 = \frac{1}{zt_A} - \frac{n_A^0 + 1}{\Delta_{A+}} - \frac{n_A^0}{\Delta_{A-}},$$

$$r_2 = \frac{1}{zt_B} - \frac{n_B^0 + 1}{\Delta_{B+}} - \frac{n_B^0}{\Delta_{B-}}, \quad (3)$$

where

$$\Delta_{A(B)+} = -\mu_{A(B)} + U_{A(B)} n_{A(B)}^0 + U_{AB} n_{B(A)}^0,$$

$$\Delta_{A(B)-} = \mu_{A(B)} - U_{A(B)} (n_{A(B)}^0 - 1) - U_{AB} n_{B(A)}^0, \quad (4)$$

which denote the particle and hole excitation energy of the species $A(B)$. The occupation numbers $n_{A(B)}^0$ are defined as the smallest integer larger than $\frac{U_{AB}(U_{AB} - U_{B(A)} - 2\mu_{B(A)}) + 2\mu_{A(B)}U_{B(A)}}{2(U_{A(B)}U_{B(A)} - U_{AB}^2)}$. The equations $r_1 = 0$ and $r_2 = 0$ generate the mean-field phase boundaries in Fig. 1. Furthermore, the two-species Bose-Hubbard model obeys a $U(1) \times U(1)$ gauge symmetry, which implies that the model is invariant under the transformation $b_\alpha(\tau) \rightarrow b_\alpha(\tau)e^{i\theta_\alpha(\tau)}$, $\phi_\alpha(\tau) \rightarrow \phi_\alpha(\tau)e^{i\theta_\alpha(\tau)}$, and

$\mu_\alpha \rightarrow \mu_\alpha + i\partial_\tau \theta_\alpha(\tau)$, where $\alpha = A, B$. This gauge invariance helps to fix the coefficients of the first- and second-order time derivatives as [35] $u_1 = -\frac{1}{t_A^2} \frac{\partial t_A}{\partial \mu_A}$, $u_2 = -\frac{1}{t_B^2} \frac{\partial t_B}{\partial \mu_B}$, $v_1 = \frac{1}{t_A^3} \left(\frac{\partial t_A}{\partial \mu_A} \right)^2 - \frac{1}{2t_A^2} \frac{\partial^2 t_A}{\partial \mu_A^2}$, and $v_2 = \frac{1}{t_B^3} \left(\frac{\partial t_B}{\partial \mu_B} \right)^2 - \frac{1}{2t_B^2} \frac{\partial^2 t_B}{\partial \mu_B^2}$, where partial derivatives $\partial t_{A(B)}/\partial \mu_{A(B)}$ and $\partial^2 t_{A(B)}/\partial \mu_{A(B)}^2$ can be calculated from Eq. (3) for fixed r_i . Along the mean-field phase boundaries the parameters u_1 and u_2 can be expressed as

$$u_1 = \frac{z(n_A^0 + 1)}{\Delta_{A+}^2} - \frac{zn_A^0}{\Delta_{A-}^2},$$

$$u_2 = \frac{z(n_B^0 + 1)}{\Delta_{B+}^2} - \frac{zn_B^0}{\Delta_{B-}^2}. \quad (5)$$

It's straightforward to see that at the tips of the insulating lobes coefficients u_1 and u_2 vanish. For simplicity we consider the QCPs at the tips of the insulating lobes; then the action of Eq. (2) is deduced to a relativistic theory. This also reflects the particle-hole symmetry at the tips of the insulating lobes. For example, we take the insulating lobes of $n_A^0 = n_B^0 = 1$. Using Eq. (5) we obtain

$$\mu_A(\mu_B) = U_A(U_B)/(\sqrt{2} + 1) + U_{AB}, \quad (6)$$

for $u_1 = u_2 = 0$. With this relations we can fine-tune the system around the tips of the lobes. In the harmonic trap this condition locates a shell in the cloud of gas. By varying the optical potential depth we will be able to change the hopping term t_α so that the system can go across the phase-transition point. Furthermore, the interaction couplings can also be calculated as

$$g_1 = \frac{2(n_A^{(0)} + 1)^2}{\Delta_{A+}^3} + \frac{2(n_A^{(0)})^2}{\Delta_{A-}^3} + \frac{(n_A^{(0)} + 1)n_A^{(0)}}{\Delta_{A+}\Delta_{A-}} \left(\frac{1}{\Delta_{A+}} + \frac{1}{\Delta_{A-}} \right),$$

$$g_2 = \frac{2(n_B^{(0)} + 1)^2}{\Delta_{B+}^3} + \frac{2(n_B^{(0)})^2}{\Delta_{B-}^3} + \frac{(n_B^{(0)} + 1)n_B^{(0)}}{\Delta_{B+}\Delta_{B-}} \left(\frac{1}{\Delta_{B+}} + \frac{1}{\Delta_{B-}} \right),$$

$$\begin{aligned}
 g_3 = & \frac{(n_A^{(0)} + 1)(n_B^{(0)} + 1)}{\Delta_{A+}\Delta_{B+}} \left(\frac{1}{\Delta_{A+}} + \frac{1}{\Delta_{B+}} \right) + \frac{n_A^{(0)}n_B^{(0)}}{\Delta_{A-}\Delta_{B-}} \left(\frac{1}{\Delta_{A-}} + \frac{1}{\Delta_{B-}} \right) \\
 & + \frac{(n_A^{(0)} + 1)n_B^{(0)}}{\Delta_{A+}\Delta_{B-}} \left(\frac{1}{\Delta_{A+}} + \frac{1}{\Delta_{B-}} \right) + \frac{(n_B^{(0)} + 1)n_A^{(0)}}{\Delta_{A-}\Delta_{B+}} \left(\frac{1}{\Delta_{A-}} + \frac{1}{\Delta_{B+}} \right). \quad (7)
 \end{aligned}$$

In the above equations we ignore the processes of two-particle or two-hole excitations of one species, since the one-particle and one-hole excitation are dominant.

III. COLEMAN-WEINBERG EFFECTIVE POTENTIAL

At the tips of the insulating lobes the classical potential of this theory is posed right on the edge of the symmetry breaking, that is $r_1 = r_2 = 0$ in Eq. (2). We wonder whether the quantum fluctuations will break the symmetry or not. To answer this question we implement the Weinberg and Coleman's effective potential method [6] to calculate the quantum corrections to the action of Eq. (2).

The notion of the effective potential has been found to be very useful in theories exhibiting spontaneously broken symmetry. It allows one to calculate quantum corrections to the classical picture of spontaneous symmetry breaking. This method is often useful in the case with the presence of a classical external field. For instance, a theory with a mean-field and quantum fluctuations. The effective potential method was first developed in high-energy physics [6]. However, it's also widely used in condensed-matter theories.

Basically, we expand the field in terms of its mean value and quantum fluctuations. Then we can integrate out the quantum fluctuations to obtain an effective theory of the mean field. All the quantum properties are incorporated in this effective theory. The nature of the effective potential can be totally different from the classical one. For example, the phase transition can be changed from second order to first order [10–17].

To obtain the effective potential we expand the fields φ_1 and φ_2 in Eq. (2) in terms of their mean fields and quantum fluctuations $\varphi_1 \rightarrow \phi_1 + \delta\phi_1$ and $\varphi_2 \rightarrow \phi_2 + \delta\phi_2$ and keep the fluctuation up to the second order. Then the action can be written as

$$S[\phi_1, \phi_2] = S_0[\phi_1, \phi_2] + \frac{1}{2} \int d\tau d^3x \delta\Phi^\dagger \mathcal{G}^{-1} \delta\Phi, \quad (8)$$

where $S_0[\phi_1, \phi_2] = \int d\tau d^3x \{ |\partial_\tau \phi_1|^2 + |\nabla \phi_1|^2 + |\partial_\tau \phi_2|^2 + |\nabla \phi_2|^2 + \frac{g_1}{2} |\phi_1|^4 + \frac{g_2}{2} |\phi_2|^4 + g_3 |\phi_1|^2 |\phi_2|^2 \}$. The parameters $v_1, w_1, v_2,$ and w_2 have been absorbed into the coordinates. Field $\delta\Phi^\dagger = [\delta\phi_1^*, \delta\phi_1, \delta\phi_2^*, \delta\phi_2]$ and $\delta\Phi$ is its Hermitian conjugate. The matrix \mathcal{G}^{-1} is

$$\begin{pmatrix}
 -\partial^2 + 2g_1\phi_1^*\phi_1 + g_3\phi_2^*\phi_2 & g_1\phi_1\phi_1 & g_3\phi_1\phi_2^* & g_3\phi_1\phi_2 \\
 g_1\phi_1^*\phi_1^* & -\partial^2 + 2g_1\phi_1^*\phi_1 + g_3\phi_2^*\phi_2 & g_3\phi_1^*\phi_2^* & g_3\phi_1^*\phi_2 \\
 g_3\phi_1^*\phi_2 & g_3\phi_1\phi_2 & -\partial^2 + 2g_2\phi_2^*\phi_2 + g_3\phi_1^*\phi_1 & g_2\phi_2\phi_2 \\
 g_3\phi_1^*\phi_2^* & g_3\phi_1\phi_2^* & g_2\phi_2^*\phi_2^* & -\partial^2 + 2g_2\phi_2^*\phi_2 + g_3\phi_1^*\phi_1
 \end{pmatrix}, \quad (9)$$

where $\partial^2 = \partial_\tau^2 + \nabla^2$.

After we integrate out the fluctuation fields $\delta\Phi$ the effective potential of our action up to one-loop level can be calculated as

$$\begin{aligned}
 V_{\text{eff}} = & g_1/2(\phi_1^*\phi_1)^2 + g_2/2(\phi_2^*\phi_2)^2 + g_3\phi_1^*\phi_1\phi_2^*\phi_2 + \frac{1}{64\pi^2} \{ m_1^4 \ln m_1^2 + m_2^4 \ln m_2^2 + m_+^4 \ln m_+^2 + m_-^4 \ln m_-^2 \} \\
 & + B_1|\phi_1|^2 + B_2|\phi_2|^2 + C_1|\phi_1|^4 + C_2|\phi_2|^4 + C_3|\phi_1|^2|\phi_2|^2, \quad (10)
 \end{aligned}$$

where

$$\begin{aligned}
 m_1^2 = & g_1|\phi_1|^2 + g_3|\phi_2|^2, \quad m_2^2 = g_2|\phi_2|^2 + g_3|\phi_1|^2, \quad m_\pm^2 = \frac{1}{2}[(3g_1 + g_3)|\phi_1|^2 + (3g_2 + g_3)|\phi_2|^2 \\
 & \pm \sqrt{[(3g_1 - g_3)|\phi_1|^2 - (3g_2 - g_3)|\phi_2|^2]^2 + 16g_3^2|\phi_1|^2|\phi_2|^2}]. \quad (11)
 \end{aligned}$$

The terms with coefficients $B_1, B_2, C_1, C_2,$ and C_3 in Eq. (10) are the renormalization counterterms. They can be fixed by imposing the renormalization conditions $\frac{\partial V_{\text{eff}}}{\partial \phi_1^* \partial \phi_1} \Big|_{\phi_1=0, \phi_2=0} = 0, \frac{\partial V_{\text{eff}}}{\partial \phi_2^* \partial \phi_2} \Big|_{\phi_1=0, \phi_2=0} = 0, V_{\text{eff}}(|\phi_1| = M, |\phi_2| = 0) = \frac{g_1}{2} M^4, V_{\text{eff}}(|\phi_1| = 0, |\phi_2| = M) = \frac{g_2}{2} M^4,$ and $V_{\text{eff}}(|\phi_1| = M, |\phi_2| = M) = (\frac{g_1}{2} + \frac{g_2}{2} + g_3) M^4,$ where M is the renormalization parameter and can be chosen arbitrarily.

The minima of the effective potential actually give the true vacuum states with the quantum fluctuation corrections.

Compared with the classical potential where the vacuum is right at the origin, the one-loop effective potential in Eq. (10) exhibits new vacua away from the origin. This can be shown in the three-dimensional and contour plots of the effective potential in Fig. 2. Without loss of generality we already simplified the effective potential by fixing the complex fields to their real directions so that the effective potential can be easily visualized in Fig. 2. That is, we take $\phi_1 \rightarrow \phi_{1R}$ and $\phi_2 \rightarrow \phi_{2R}$. ϕ_{1R} and ϕ_{2R} are real fields. Here we take the parameters $g_1 < g_2$ in different values; then we observe that the new

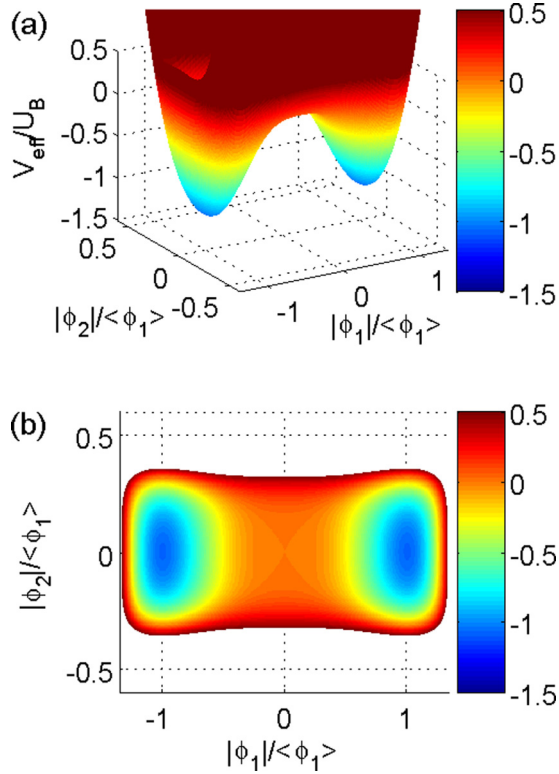


FIG. 2. (Color online) Three-dimensional and contour plots of the effective potential of the two-species Bose-Hubbard model. Coefficients $r_1 = r_2 = 0$ for both graph (a) and (b). We use U_B as the energy scale to make all the couplings dimensionless. Here we take $U_B/U_A = 0.3$, then the interaction couplings are $g_2 U_B^3 = 101.9$ and $g_3 U_B^3 = 26.5$. We take renormalization parameter $M = \langle \phi_1 \rangle$, where $\langle \phi_1 \rangle$ is the vacuum of field ϕ_1 . The interaction coupling g_1 is eliminated by the condition $\frac{\partial V_{\text{eff}}}{\partial \phi_1} |_{\phi_1 = \langle \phi_1 \rangle} = 0$.

vacua appear at $\phi_1^* \phi_1 \neq 0, \phi_2^* \phi_2 = 0$ in Figs. 2(a) and 2(b). Hence the $U(1) \times U(1)$ symmetry is spontaneously broken to $U(1)$ symmetry. At the new vacuum the field ϕ_2 stays in the insulator phase and field ϕ_1 is in the superfluid phase. Notice that in Fig. 2 we choose renormalization parameter $M = \langle \phi_1 \rangle$ since M is arbitrary, where $\langle \phi_1 \rangle$ is the vacuum of field ϕ_1 . By setting $M = \langle \phi_1 \rangle$ the interaction coupling g_1 is eliminated through the condition $\frac{\partial V_{\text{eff}}}{\partial \phi_1} |_{\phi_1 = \langle \phi_1 \rangle} = 0$. Here we introduce a dimensional parameter $\langle \phi_1 \rangle$ and eliminate a dimensionless one g_1 . This is called the dimensional transmutation [6].

However, the appearance of new vacua can be an artifact since the new vacua may lie outside the range of validity of the one-loop approximation [6]. In order to investigate the validity of our result we take the direction of $\phi_2^* \phi_2 = 0$ in the effective potential to explore the vacuum. Along this direction the effective potential can be reduced to

$$V_{\text{eff}} = g_1/2(\phi_1^* \phi_1)^2 + \frac{1}{32\pi^2} g_3^2 (\phi_1^* \phi_1)^2 \ln \frac{\phi_1^* \phi_1}{M^2}. \quad (12)$$

The effective potential of Eq. (12) includes a term of $\ln \frac{\phi_1^* \phi_1}{M^2}$. The logarithm of a small number is negative. Hence the minimum arose from balancing a term of order g_1 against a term of order $g_3^2 \ln \frac{\phi_1^* \phi_1}{M^2}$. Even though the second term

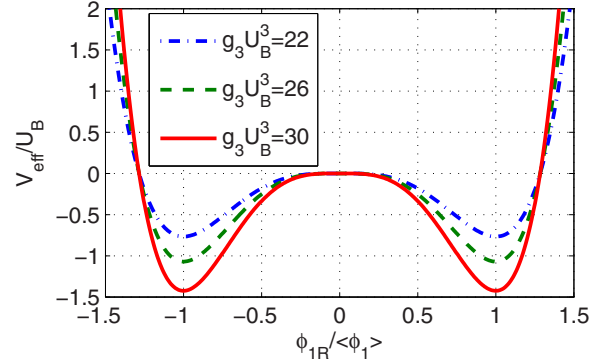


FIG. 3. (Color online) Effective potential along the $\phi_2^* \phi_2 = 0$ direction with different values of g_3 . The parameters are $r_1 = r_2 = 0$ and $g_2 U_B^3 = 101.9$. g_3 is indicated in the graph. We take renormalization parameter $M = \langle \phi_1 \rangle$. The interaction coupling g_1 is eliminated by the condition $\frac{\partial V_{\text{eff}}}{\partial \phi_1} |_{\phi_1 = \langle \phi_1 \rangle} = 0$.

formally arises in a higher order of our expansion, there is no reason why g_1 cannot be of the same order of magnitude as g_3^2 . In the realistic system the coupling constant g_1 and g_3 can be calculated through Eq. (7). With the condition Eq. (6) we can derive the couplings approximately as $g_1 \sim \frac{1}{U_A}$ and $g_3 \sim \frac{1}{U_A U_B} (\frac{1}{U_A} + \frac{1}{U_B})$. If we tune $U_A \gg U_B$ we can have $g_3^2 \gg g_1$. Hence our result is inside the range of validity of the one-loop approximation. The new vacuum is illustrated in Fig. 3. As g_3 gets stronger the vacuum becomes deeper.

The excitation spectrum around the new vacuum can be calculated by expanding the effective action around the new vacuum of $|\phi_1|^2 = \rho$, $|\phi_2|^2 = 0$. Let us write $\phi_1 \rightarrow \sqrt{\rho} + \delta\phi_1$, $\phi_2 \rightarrow \delta\phi_2$. Up to the quadratic order of the fields $\delta\phi_1$ and $\delta\phi_2$ a straightforward computation yields $S = \int d\tau d^3x \{ |\partial_\tau \delta\phi_1|^2 + |\nabla \delta\phi_1|^2 + |\partial_\tau \delta\phi_2|^2 + |\nabla \delta\phi_2|^2 - \frac{g_3^2}{64\pi^2} \rho^2 + \frac{g_3^2}{32\pi^2} \rho (\delta\phi_1^2 + \delta\phi_1^{*2} + 2\delta\phi_1^* \delta\phi_1) + g_3 \rho \delta\phi_2^* \delta\phi_2 \}$. The diagonalization of the mass term of field $\delta\phi_1$ generates two mass eigenvalues $m_1^2 = \frac{g_3^2}{16\pi^2} \rho$ or 0. The massless excitation is the Goldstone mode, which indicates the breakdown of $U(1)$ symmetry of field ϕ_1 . The field $\delta\phi_2$ has two modes with the same mass $m_2^2 = g_3 \rho$.

IV. NATURE OF THE PHASE TRANSITION

We investigate the effective potential with nonzero parameter r_1 and r_2 . For large enough r_1 and r_2 the vacuum of the effective potential is at the origin. Now we vary the coefficient r_1 to study how the vacuum changes. Along the direction of $\phi_2^* \phi_2 = 0$ the effective potential is obtained as $V_{\text{eff}} = r_1 |\phi_1|^2 + \frac{g_1}{2} |\phi_1|^4 + \frac{(r_2 + g_3 |\phi_1|^2)^2}{32\pi^2} \ln(r_2 + g_3 |\phi_1|^2) - \frac{r_2^2 \ln r_2}{32\pi^2} - \frac{(\phi_1^* \phi_1)^2}{32\pi^2 M^4} (r_2 + g_3 M^2)^2 \ln(r_2 + g_3 M^2)$. Here if we choose the value of r_1 small enough a local minimum will appear away from the origin as show in Fig. 4(a). For simplicity we take the renormalization parameter $M^2 = \langle \phi_1 \rangle^2$, where $\langle \phi_1 \rangle$ is the average value of the field ϕ_1 at the local minimum. Using the condition of $\frac{\partial V_{\text{eff}}}{\partial \phi_1} |_{\phi_1 = \langle \phi_1 \rangle} = 0$ the

effective potential can be simplified as

$$V_{\text{eff}} = r_1 |\phi_1|^2 + \frac{(r_2 + g_3 |\phi_1|^2)^2}{32\pi^2} \ln(r_2 + g_3 |\phi_1|^2) + \frac{(\phi_1^* \phi_1)^2}{2 \langle \phi_1 \rangle^2} \left(-r_1 - \frac{g_3(r_2 + g_3 \langle \phi_1 \rangle^2)}{16\pi^2} \ln(r_2 + g_3 \langle \phi_1 \rangle^2) - \frac{g_3}{32\pi^2} (r_2 + g_3 \langle \phi_1 \rangle^2) \right) - \frac{r_2^2 \ln r_2}{32\pi^2}. \quad (13)$$

As we lower the parameter r_1 the vacuum of the above effective potential jumps from the origin to a new vacuum at $\phi_1^* \phi_1 = \langle \phi_1 \rangle^2$ and $\phi_2^* \phi_2 = 0$, where the type A bosons become superfluid and type B bosons stay in the insulator phase. This phase transition occurs at a finite value of r_1 . The change of the vacuum is shown in graph (a) of Fig. 4. As r_1 approaches to the critical value r_{1c} there is a first-order phase transition, where critical value of r_1 is

$$r_{1c} = \frac{1}{16\pi^2 \langle \phi_1 \rangle^2} r_2^2 \ln r_2 + \frac{g_3}{32\pi^2} (r_2 + g_3 \langle \phi_1 \rangle^2) - \frac{r_2}{16\pi^2 \langle \phi_1 \rangle^2} (r_2 + g_3 \langle \phi_1 \rangle^2) \ln(r_2 + g_3 \langle \phi_1 \rangle^2). \quad (14)$$

In graph (b) of Fig. 4 we show the dependence of r_{1c} on the parameter r_2 . As r_2 gets larger the critical value r_{1c} becomes smaller and even goes to zero, where the second-order phase

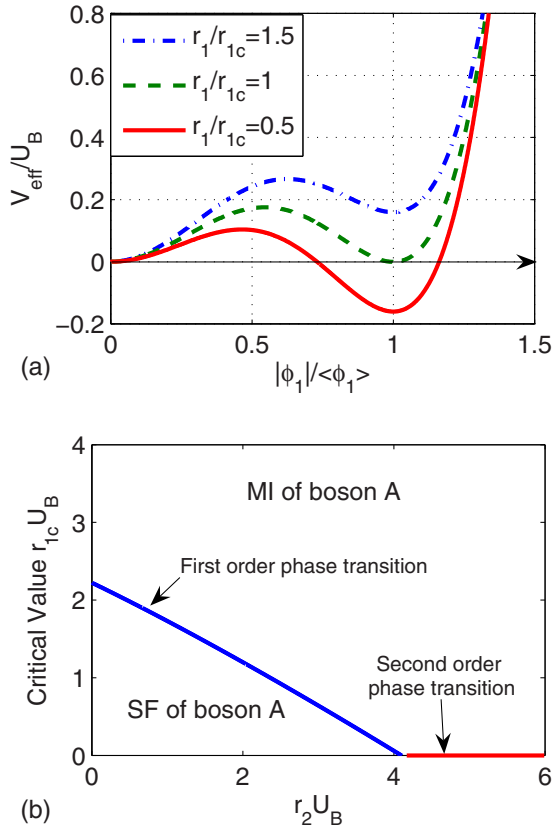


FIG. 4. (Color online) (a) Effective potential along the $\phi_2^* \phi_2 = 0$ direction with different values of r_1 , where $r_2 U_B = 3$, $g_2 U_B^3 = 101.9$, $g_3 U_B^3 = 26.5$, and $r_{1c} U_B \simeq 0.64$. (b) The critical value r_{1c} of the first-order phase transition of type A bosons as a function of coefficient r_2 .

transition will take place. That is, if the field ϕ_2 is deeply in the insulator phase the first-order phase transition of ϕ_1 cannot be induced. This quantum fluctuation-driven first-order phase transition can only happen near the QCP with the appearance of competing orders.

At a first-order phase transition certain physical quantities, such as the order parameter and the energy density, have a discontinuous behavior and the correlation lengths remain generally finite. Hence there is no true critical behavior. However, it turns out to be useful to develop a scaling approach for these transitions [36,37] with scaling exponents such as $\beta = 0$, $\alpha = \gamma = 1$, $\nu = 1/(d+z)$, and $\delta = \infty$. In our case the effective potential at the metastable minimum $\phi_1^* \phi_1 = \langle \phi_1 \rangle^2$ can be written as $V_{\text{eff}}(\langle \phi_1 \rangle) = 1/2(r_1 - r_{1c}) \langle \phi_1 \rangle^2$. Introducing a parameter $\delta = r_1 - r_{1c}$ which measures the distance to the critical value r_{1c} , we have $V_{\text{eff}} \propto |\delta|^{2-\alpha}$. We can identify that $\alpha = 1$, which reflects the nature of the phase transition, is first order.

The finite temperature case can be studied through replacing the frequency integrations in the calculation of the effective potential by sums over the Matsubara frequencies. With high-temperature approximation $T \gg r_{1c}$ the effective potential is written as $V_{\text{eff}} = V_{\text{eff}}(T=0) - \frac{2\pi^2}{45} T^4 + [r_1 + r_2 + (2g_1 + g_3)\phi_1^* \phi_1] \frac{T^2}{12}$, where $V_{\text{eff}}(T=0)$ is the effective potential in Eq. (13) and we take $k_B = 1$. The first-order phase transition at finite temperature occurs at $r_1 + \frac{T^2}{12}(2g_1 + g_3) = r_{1c}$, where r_{1c} is the critical value in Eq. (14). Then the critical temperature of the first-order phase transition is

$$T_c = \sqrt{\frac{12(r_{1c} - r_1)}{2g_1 + g_3}}. \quad (15)$$

Furthermore, at high temperature the effective potential at the metastable minimum can be cast in a scaling form

$$V_{\text{eff}} = \frac{1}{2} |\delta|^{2-\alpha} \langle \phi_1 \rangle^2 \left(1 - \frac{4\pi^2 T^4}{45 |\delta| \langle \phi_1 \rangle^2} \right) = |\delta|^{2-\alpha} F \left[\frac{T}{T_X} \right], \quad (16)$$

where the crossover line is $T_X = |\delta|^{\nu} = |\delta|^{\frac{1}{4}}$. We can identify that $\nu = 1/4$ with $z = 1$ in our case. This satisfies the hyperscaling relation $2 - \alpha = \nu(d+z)$ and the universality of first-order phase transition, where $\nu = \frac{1}{d+z}$ [37]. Finite-temperature phase diagram is shown in Fig. 5.

V. EXPERIMENTAL PROPOSALS

The study of quantum criticality in cold-atom systems is based on *in situ* density measurements [1–3,5]. General arguments show that the observables obey universal scaling relations near the QCPs. The density can be cast as $n(\mu, T) - n_r(\mu, T) = T^{\frac{d}{z}+1-\frac{1}{\nu}} G(\frac{\mu-\mu_c}{T^{1/z\nu}})$, where μ_c is the critical value of

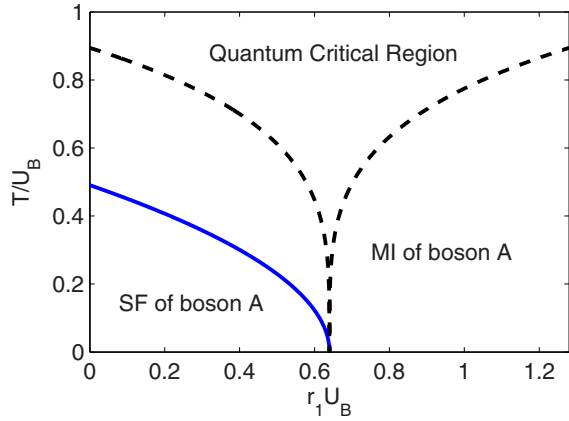


FIG. 5. (Color online) Phase diagram of type A bosons at finite temperature. The parameters are set as $r_2 U_B = 3$, $g_2 U_B^3 = 101.9$, and $g_3 U_B^3 = 26.5$. T_c is the critical line of the first-order phase transition of boson A . T_X is the crossover line.

the chemical potential, n_r is the regular part of the density, and $G(x)$ is a universal function describing the singular part of the density. Following the scheme developed by Zhou and Ho [1] we can plot the “scaled density” $A(\mu, T) \equiv T^{-\frac{d}{z}-1+\frac{1}{\tilde{\nu}}}[n(\mu, T) - n_r]$ versus $(\mu - \mu_c)/T^{\frac{1}{\tilde{\nu}}}$. The scaled density curves for all temperatures will collapse into a single curve. Here it’s important to notice that our calculation of $\nu = \frac{1}{4}$ is with respect to the argument $\delta = r_1 - r_{1c}$. However, in the realistic cold-atom experiments we use $\mu_1 - \mu_{1c}$ to measure the distance to the QCP. Hence a critical exponent $\tilde{\nu}$ with respect to the argument $\mu_1 - \mu_{1c}$ should be obtained.

As we approach the tip of the insulator lobe by varying the chemical potential we have [33] $\delta = r_1 - r_{1c} \sim (\mu_1 - \mu_{1c})^2$. A straightforward calculation yields $\tilde{\nu} = 2\nu = \frac{1}{2}$. Then the scaled density will be in the form of $A(\mu, T) = T^{-2}[n(\mu, T) - n_r]$ near the first-order QCP, where we have $z = 1$, $d = 3$, and $\tilde{\nu} = \frac{1}{2}$. In order to distinguish this case from the second-order phase transition we also calculate the scaled density near the second-order QCP, which belongs to the three-dimensional XY universality class with critical exponents $z = 1$ and $\tilde{\nu} = 1$ [33]. Then the scaled density is $A(\mu, T) = T^{-3}[n(\mu, T) - n_r]$. By testing which form the measured scaled density obeys we can determine whether the phase transition is in first or second order.

VI. CONCLUSIONS

In summary, we have investigated the quantum fluctuation effects in two-species bosons in a three-dimensional optical lattice. We find that nature of the superfluid-Mott insulator phase transition of one type of bosons can be changed from second order to first order by the quantum fluctuations of the other type of bosons. The scaling behavior of this first-order phase transition was studied and the critical exponents were calculated. Finally, we discussed the observation of this phenomenon in a realistic cold-atom experiment.

ACKNOWLEDGMENTS

It’s a pleasure to thank Hui Zhai, Tin-Lun Ho, Xiao-Lu Yu, and Zhenhua Yu for useful discussions. This work is supported by the NKBRSCF under Grant No. 2012CB821400 and NSFC under Grant No. 1190024.

-
- [1] Q. Zhou and T.-L. Ho, *Phys. Rev. Lett.* **105**, 245702 (2010).
 [2] K. R. A. Hazzard and E. J. Mueller, *Phys. Rev. A* **84**, 013604 (2011).
 [3] X. Zhang, C.-L. Hung, S.-K. Tung, N. Gemelke, and C. Chin, *New J. Phys.* **13**, 045011 (2011).
 [4] T. Donner, S. Ritter, T. Bourdel, A. Öttl, M. Köhl, and T. Esslinger, *Science* **315**, 1556 (2007).
 [5] X. Zhang, C.-L. Hung, S.-K. Tung, and C. Chin, *Science* **335**, 1070 (2012).
 [6] S. Coleman and E. Weinberg, *Phys. Rev. D* **7**, 1888 (1973).
 [7] B. I. Halperin, T. C. Lubensky, and S.-K. Ma, *Phys. Rev. Lett.* **32**, 292 (1974).
 [8] D. J. Amit, *Field Theory, the Renormalization Group, and Critical Phenomena*, 2nd ed. (World Scientific, Singapore, 1984), Part II, Chap. 4.
 [9] C. Domb and M. S. Green, *Phase Transition and Critical Phenomena* (Academic Press, London, 1976), Vol. 6, Chap. 6.
 [10] M. A. Continentino and A. S. Ferreira, *Physica A* **339**, 461 (2004).
 [11] A. S. Ferreira, M. A. Continentino, and E. C. Marino, *Phys. Rev. B* **70**, 174507 (2004).
 [12] K. Yang, *Phys. Rev. B* **77**, 085115 (2008).
 [13] Y. Qi and C. Xu, *Phys. Rev. B* **80**, 094402 (2009).
 [14] A. J. Millis, *Phys. Rev. B* **81**, 035117 (2010).
 [15] J.-H. She, J. Zaanen, A. R. Bishop, and A. V. Balatsky, *Phys. Rev. B* **82**, 165128 (2010).
 [16] S. Diehl, M. Baranov, A. J. Daley, and P. Zoller, *Phys. Rev. Lett.* **104**, 165301 (2010).
 [17] L. Bonnes and S. Wessel, *Phys. Rev. Lett.* **106**, 185302 (2011).
 [18] J. Catani, L. DeSarlo, G. Barontini, F. Minardi, and M. Inguscio, *Phys. Rev. A* **77**, 011603(R) (2008).
 [19] S. Trotzky *et al.*, *Science* **319**, 295 (2008).
 [20] G. Thalhammer, G. Barontini, L. De Sarlo, J. Catani, F. Minardi, and M. Inguscio, *Phys. Rev. Lett.* **100**, 210402 (2008).
 [21] B. Gadway, D. Pertot, R. Reimann, and D. Schneble, *Phys. Rev. Lett.* **105**, 045303 (2010).
 [22] J. R. Han, T. Zhang, Y. Z. Wang, and W. M. Liu, *Phys. Lett. A* **332**, 131 (2004).
 [23] P. Buonsante, S. M. Giampaolo, F. Illuminati, V. Penna, and A. Vezzani, *Phys. Rev. Lett.* **100**, 240402 (2008).
 [24] G. H. Chen and Y. S. Wu, *Phys. Rev. A* **67**, 013606 (2003).
 [25] A. Isacson, M. C. Cha, K. Sengupta, and S. M. Girvin, *Phys. Rev. B* **72**, 184507 (2005).
 [26] Y. Li, M. R. Bakhtiari, L. He, and W. Hofstetter, *Phys. Rev. A* **85**, 023624 (2012).
 [27] E. Altman, W. Hofstetter, E. Demler, and M. D. Lukin, *New J. Phys.* **5**, 113 (2003).

- [28] A. B. Kuklov and B. V. Svistunov, *Phys. Rev. Lett.* **90**, 100401 (2003).
- [29] A. Kuklov, N. Prokof'ev, and B. Svistunov, *Phys. Rev. Lett.* **92**, 050402 (2004).
- [30] M. Greiner, O. Mandel, T. Esslinger, T. W. Hänsch, and I. Bloch, *Nature (London)* **415**, 39 (2002).
- [31] T. Stöferle, H. Moritz, C. Schori, M. Köhl, and T. Esslinger, *Phys. Rev. Lett.* **92**, 130403 (2004).
- [32] I. B. Spielman, W. D. Phillips, and J. V. Porto, *Phys. Rev. Lett.* **98**, 080404 (2007).
- [33] M. P. A. Fisher, P. B. Weichman, G. Grinstein, and D. S. Fisher, *Phys. Rev. B* **40**, 546 (1989).
- [34] D. Jaksch, C. Bruder, J. I. Cirac, C. W. Gardiner, and P. Zoller, *Phys. Rev. Lett.* **81**, 3108 (1998).
- [35] S. Sachdev, *Quantum Phase Transition* (Cambridge University Press, Cambridge, UK, 2011).
- [36] B. Nienhuis and N. Nauenberg, *Phys. Rev. Lett.* **35**, 477 (1975).
- [37] M. E. Fisher and A. N. Berker, *Phys. Rev. B* **26**, 2507 (1982).